

# THE EFFECT OF MASS-SEGREGATION ON GRAVITATIONAL WAVE SOURCES NEAR MASSIVE BLACK HOLES

CLOVIS HOPMAN AND TAL ALEXANDER<sup>1</sup>

Faculty of Physics, Weizmann Institute of Science, POB 26, Rehovot 76100, Israel

*Draft version 28th August 2018*

## Abstract

Gravitational waves (GWs) from the inspiral of compact remnants (CRs) into massive black holes (MBHs) will be observable to cosmological distances. While a CR spirals in, 2-body scattering by field stars may cause it to fall into the MBH before reaching a short period orbit that would give an observable signal. As a result, only CRs very near ( $\sim 0.01$  pc) the MBH can spiral in successfully. In a multi-mass stellar population, the heaviest objects sink to the center, where they are more likely to slowly spiral into the MBH without being swallowed prematurely. We study how mass-segregation modifies the stellar distribution and the rate of GW events. We find that the inspiral rate per galaxy for white dwarfs is  $30 \text{ Gyr}^{-1}$ , for neutron stars  $6 \text{ Gyr}^{-1}$ , and for stellar black holes (SBHs)  $250 \text{ Gyr}^{-1}$ . The high rate for SBHs is due to their extremely steep density profile,  $n_{\text{BH}}(r) \propto r^{-2}$ . The GW detection rate will be dominated by SBHs.

*Subject headings:* black hole physics — stellar dynamics — gravitational waves — Galaxy: center

## 1. INTRODUCTION

Massive Black Holes (MBHs) with masses  $M_{\bullet} \lesssim 5 \times 10^6 M_{\odot}$  have Schwarzschild radii  $r_S = 2GM_{\bullet}/c^2$ , such that a test mass orbiting at a few  $r_S$  emits gravitational waves (GWs) with frequencies  $10^{-4} \text{ Hz} \lesssim \nu \lesssim 1 \text{ Hz}$ , detectable by the planned space based *Laser Interferometer Space Antenna*<sup>2</sup> (*LISA*). Main sequence (MS) stars with mass  $M_{\star}$  and radius  $R_{\star}$  will be disrupted at the tidal radius  $r_t = (M_{\bullet}/M_{\star})^{1/3} R_{\star} > r_S$  and are therefore unlikely to be sources of observable GWs (our own Galactic center may be an exception, Freitag 2003). Compact remnants (CRs) such as white dwarfs (WDs), neutron stars (NSs) and stellar black holes (SBHs) have tidal radii  $r_t < r_S$  and can emit GWs that are observable to cosmological distances. The inspiral of a CR into a MBH (“extreme mass ratio inspiral sources” [EMRIs]) is among the main targets of *LISA*.

The event rate of EMRIs has been estimated by numerous authors (Hils & Bender 1995; Sigurdsson & Rees 1997; Miralda-Escudé & Gould 2000; Freitag 2001; Ivanov 2002; Freitag 2003; Alexander & Hopman 2003; Hopman & Alexander 2005, 2006) but remains rather uncertain, in part because of the slow nature of the inspiral process, which occurs on many dynamical times. This makes the inspiraling star very susceptible to scattering by other stars, which can change the orbital parameters. The formalism for inspiral rates is similar to that for prompt consumption of stars (Bahcall & Wolf 1977; Lightman & Shapiro 1977; Frank & Rees 1976; Cohn & Kulsrud 1978; Syer & Ulmer 1999; Magorrian & Tremaine 1999), but there are some important differences because the process is much slower.

The picture can be understood as follows: Let  $t_r$  be the relaxation time of a star with negative energy  $E$  (hereafter “energy”;  $E > 0$  for bound stars) and specific angular momentum  $J$  (hereafter “angular momentum”). The relaxation time is the time-scale for a change of energy of order  $E$ , or a change in angular momentum of order  $J_c(E)$ , the circular angular momentum. The change in  $J$  of a star per orbital period  $P$  is  $\Delta J = (P/t_r)^{1/2} J_c$ . The time-scale for a change of

order  $J$  is  $t_J = (J/J_c)^2 t_r$ . In particular, the time-scale for a change in  $J$  by the order of the loss-cone, determined by the angular momentum of the last stable orbit  $J_{\text{LSO}} = 4GM_{\bullet}/c$ , is  $t_{lc} = (J_{\text{LSO}}/J_c)^2 t_r$ . Inspiral due to dissipation by GW emission happens on a time-scale  $t_0(E, J)$ , which for highly eccentric orbits has a very strong angular momentum dependence,  $t_0(J) \propto J^7$ . If  $t_{lc} \ll t_0(E, J \rightarrow J_{\text{LSO}})$ , the angular momentum will be modified even if the star has  $J \gtrsim J_{\text{LSO}}$ . As a result it is very likely that the star will be scattered into the loss-cone (or away from it, to an orbit where energy dissipation is very weak). Such CRs will eventually be consumed by the MBH and add to its mass, but they will not be observable as GW emitters (GW bursts in our own GC may form an exception [Rubbo, Holley-Bockelmann & Finn 2006]).

The approximate condition  $t_0(E, J \rightarrow J_{\text{LSO}}) < t_{lc}(E)$  translates into a minimal energy or maximal semi-major axis  $a_{\text{GW}}$  a CR must have in order to spiral in and become a *LISA* source (“successful inspiral”); Hopman & Alexander (2005; hereafter HA05) estimate that for a MBH of  $M_{\bullet} = 3 \times 10^6 M_{\odot}$ ,  $a_{\text{GW}} \sim 0.01$  pc: nearly all CRs with  $a \gg a_{\text{GW}}$  are promptly captured or deflected without giving an observable signal, while nearly all stars with  $a \ll a_{\text{GW}}$  do spiral in successfully.

The fact that the distribution of CRs near MBHs is crucial to the observational outcome, implies that mass-segregation is likely to play a very important role for EMRIs. Mass-segregation is a manifestation of dynamical friction. It drives the heaviest objects to the center, so their concentration within  $a_{\text{GW}}$  increases, and drives the lightest stars to larger radii, so that they are relatively rare within  $a_{\text{GW}}$ . The importance of mass-segregation on inspiral processes was dramatically demonstrated in  $N$ -body simulations (Baumgardt et al. 2004, 2005) of tidal capture of MS stars (Alexander & Morris 2003; Hopman et al. 2004). Baumgardt et al. (2005) studied tidal capture by a  $\sim 10^3 M_{\odot}$  black hole in a young stellar cluster with MS masses up to  $\sim 100 M_{\odot}$ . In spite of the fact that massive stars are scarce, captured stars typically had masses  $M_{\star} \sim 20 M_{\odot}$ .

In this Letter we study the implications of mass-segregation on the EMRI rate.

## 2. MODEL

<sup>1</sup> The William Z. & Eda Bess Novick career development chair

Electronic address: clovis.hopman, tal.alexander@weizmann.ac.il

<sup>2</sup> <http://lisa.jpl.nasa.gov/>

Our model is based on Bahcall & Wolf (1976, 1977). Here we briefly recapitulate the main assumptions, and discuss our treatment of GW capture. A detailed discussion of our model can be found in HA05 and Hopman & Alexander (2006).

### 2.1. Dynamics

The MBH dominates the dynamics of stars within its “Bondi radius”, or radius of influence,  $r_h = GM_\bullet/\sigma_\star^2$ , where  $\sigma_\star$  is the velocity dispersion of a typical star of mass  $M_\star \ll M_\bullet$  (assumed of Solar type), which we will use to scale our expressions. Orbits are assumed to be Keplerian within  $r_h$ . Each species with mass  $M$  is described by a distribution function (DF) in energy space  $f_M(E)$ .

We define a dimensionless time  $\tau = t/T_h$  in terms of the relaxation time at the radius of influence

$$T_h = \frac{3(2\pi\beta/M_\star)^{3/2}}{32\pi^2 G^2 M_\star^2 n_\star \ln \Lambda}, \quad (1)$$

where  $n_\star$  is the number density at  $r_h$  for the typical star  $M_\star$ ,  $\beta = M_\star\sigma_\star^2$ , and  $\Lambda = M_\bullet/M_\star$ . Introducing the dimensionless energy  $x = (M_\star/M)(E/\beta)$  and the dimensionless DF  $g_M(x) = [(2\pi\beta/M_\star)^{3/2}n_\star^{-1}]f_M(E)$ , the Fokker-Planck equation in energy space is (Bahcall & Wolf 1977 Eq. [26])

$$\frac{\partial g_M(x, \tau)}{\partial \tau} = -x^{5/2} \frac{\partial}{\partial x} Q_M(x) - R_M(x). \quad (2)$$

We also write equation (2) in a logarithmic form suitable for numerical integration (see appendix). The spatial number density  $n_M(r)$  of stars is related to the DF by

$$n_M(r) = 2\pi^{-1/2} n_\star \int_{-\infty}^{r_h/r} dx g_M(x) [r_h/r - x]^{1/2}. \quad (3)$$

We fit our numerical results by power-laws  $n_M(r) \propto r^{-\alpha_M}$ .

In expression (2),  $Q_M(x)$  is the (dimensionless) rate at which stars flow to energies larger than  $x$ ,

$$Q_M(x) = \sum_{M'} \frac{M}{M_\star} \frac{M'}{M_\star} \int_{-\infty}^{x_D} dx' [\max(x, x')]^{-3/2} \times \left[ g_M(x) \frac{\partial g_{M'}(x')}{\partial x'} - \frac{M'}{M} g_{M'}(x') \frac{\partial g_M(x)}{\partial x} \right] \quad (4)$$

The dimensional stellar current is related to  $Q_M$  by  $I_M(E, t) = I_0 Q_M(x, t)$ , where

$$I_0 \equiv \frac{8\pi^2}{3\sqrt{2}} r_h^3 n_\star \frac{(GM_\star)^2 \ln \Lambda n_\star}{\sigma_\star^3}. \quad (5)$$

(Bahcall & Wolf 1976; Hopman & Alexander 2006).

The last term in equation (2) represents losses of stars due to loss-cone effects (both prompt infall and inspiral) in  $J$ -space. The sink term in the diffusive regime for the loss-cone is

$$R_M(x) = \frac{g_M(x)}{\tau_r(x) \ln[J_c(x)/J_{\text{LSO}}]}, \quad (6)$$

where  $J_c(x)/J_{\text{LSO}} = (1/4\sqrt{2})(c/\sigma_\star)x^{-1/2}$ . The full-loss cone regime,  $x \lesssim 10$ , does not contribute to the GW event rate (Alexander & Hopman 2003; HA05; Hopman & Alexander 2006). In our calculations we neglect the sink term in the full loss-cone regime by setting  $R_M \rightarrow 0$  for  $x < 10$ . In Eq. (6) the dimensionless *local relaxation time*  $\tau_r(x)$  is

$$\tau_r(x) = \frac{M_\star^2}{\sum_M g_M(x) M^2}, \quad (7)$$

independent of the stellar mass.

Let the number of stars accreted to the MBH before giving an observable GW signal be  $N_p(x)$ , and the number of those that spiral in successfully and do give a signal  $N_i(x)$ . The steady state result for  $\tau_r(x)$  is used to determine the probability for inspiral  $S_M(x) = N_i(x)/[N_i(x) + N_p(x)]$  by Monte Carlo simulations (HA05) as follows. At every orbit, a star of initial energy  $E$  and initially large  $J$  makes a step in  $J$  of order  $\Delta J = [P(x)/t_r(x)]^{1/2} J_c$  with random sign because of scattering, and loses energy  $\Delta E_{\text{GW}} = (85\pi/24576)(M/M_\bullet) M c^2 (J/J_{\text{LSO}})^{-7}$  to GWs (Peters 1964). This is repeated many times and the outcome is recorded. The total rate of *successful inspirals* for species  $M$  is then given by  $\Gamma_M = I_0 \int_{-\infty}^{\infty} dx S_M(x) x^{-5/2} R_M(x)$ . It is convenient to express the capture rate in terms of the semi-major axis  $a = r_h/2x$  of the stars,

$$\Gamma_M(< a) = \frac{2\sqrt{2}I_0}{r_h^{3/2}} \int_0^a da a^{1/2} S_M(a) R_M(a). \quad (8)$$

### 2.2. Boundary conditions and model parameters

Equation (2) has inner and outer boundary conditions. At some large energy  $x_D$  the DF vanishes,  $g(x > x_D) = 0$ . Since the EMRI rate is dominated by the largest distance where successful capture is possible, the exact value of  $x_D$  is not important. Here we used  $x_D = 10^4$ , which is approximately the energy-scale where the inspiral time becomes smaller than a Hubble time even for a circular orbit. We assume that the MBH mass is  $M_\bullet = 3 \times 10^6 M_\odot$ , representative of a typical *LISA* source. Our value of  $x_D$  would approximately correspond to a distance scale of  $\sim 10^{-4}$  pc from the MBH.

The second boundary condition is given at  $x = 0$ : following Bahcall & Wolf (1977), we assume that for  $x < 0$  the stars have a Maxwellian velocity DF with equal temperature ( $\beta_M \equiv M\sigma_M^2 = \beta$ ), and with different population number fractions for different species  $C_M$ ,

$$g_M(x) = C_M \exp(Mx/M_\star); \quad (x < 0). \quad (9)$$

We consider four populations of stars. One species consists of main sequence stars, assumed here to be of Solar mass. MSs do not contribute to the GW inspiral rate since they are tidally disrupted before spiraling in, but they do contribute dynamically and they dominate both in number and in total mass at the radius of influence. The other three populations consists of WDs ( $M_{\text{WD}} = 0.6M_\odot$ ), NSs ( $M_{\text{NS}} = 1.4M_\odot$ ) and SBHs ( $M_{\text{BH}} = 10M_\odot$ ). The number fraction ratios of the four populations at  $x = 0$  are  $C_{\text{MS}} : C_{\text{WD}} : C_{\text{NS}} : C_{\text{BH}} = 1 : 0.1 : 0.01 : 10^{-3}$ , typical for continuously star forming populations (Alexander 2005). We also adopt for our model the Galactic center values  $\sigma_\star = 75 \text{ km s}^{-1}$  ( $r_h = 2 \text{ pc}$ ) and  $n_\star = 4 \times 10^4 \text{ pc}^{-3}$  (Genzel et al. 2003)<sup>3</sup>. The model parameters are summarized in table (1).

## 3. RESULTS

We integrated Eq. (2) until steady state is obtained, after time  $\tau \lesssim 1$ . In figure (1) we show the resulting densities for the different species. The DF of the SHBs is much steeper than that of the other types ( $\alpha_{\text{BH}} = 2.0$ ), and at

<sup>3</sup> The Galactic MBH obeys the  $M_\bullet - \sigma$  relation (Ferrarese & Merritt 2000; Gebhardt et al. 2000; Tremaine et al. 2002), so that these values may also be representative of other MBHs.

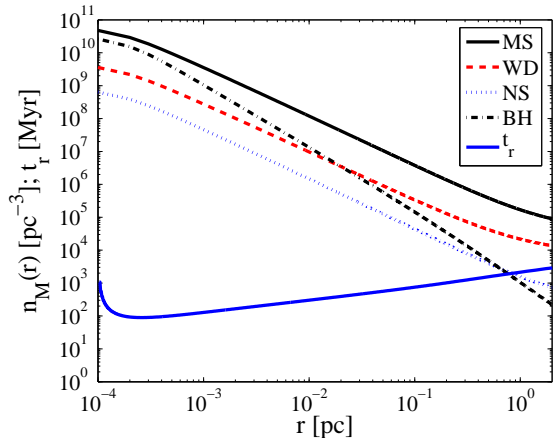


FIG. 1.— Steady state number densities  $n_M(r)$ . The DF of SBHs (dashed-dotted) is much steeper than that of the other three stars ( $\alpha_{\text{BH}} \approx 2$ ). SBHs dominate NSs (dotted) by number nearly everywhere, and they even dominate WDs (red dashed) within  $\sim 0.01$  pc, in spite of their low number fraction at  $r_h$ ,  $C_{\text{BH}}/C_{\text{WD}} = 1\%$ . MS stars (solid) dominate by number everywhere. For the other three species we found  $\{\alpha_{\text{MS}}, \alpha_{\text{WD}}, \alpha_{\text{NS}}\} = \{1.4, 1.4, 1.5\}$ . The relaxation time (rising solid line) grows approximately as  $t_r \propto r^{0.5}$ .

TABLE 1  
MODEL PARAMETERS AND GW RATES

Star	$M$ [ $M_\odot$ ]	$C_M$	$\alpha_M$	$N_M(<0.01\text{pc})$	$N_M(<0.1\text{pc})$	$a_{\text{GW}}$ [mpc]	$\Gamma_M$ [ $\text{Gyr}^{-1}$ ]
MS	1	1.0	1.4	$10^3$	$3 \times 10^4$	-	-
WD	0.6	0.1	1.4	80	$2.7 \times 10^3$	4	30
NS	1.4	0.01	1.5	12	374	5	6
SBH	10	$10^{-3}$	2.0	150	$1.8 \times 10^3$	13	250

$r \approx 0.01$  pc the number density of SBHs becomes comparable to that of the WDs. MS stars dominate everywhere by number, although we did not take into account stellar collisions (Freitag & Benz 2002, 2005) which could deplete the MSs close to the MBH. SBHs also determine the functional behavior of  $t_r \propto r^p$ , where  $p \approx \alpha_{\text{BH}} - 3/2 \approx 0.5$ .

Throughout most of the cusp  $\alpha_{\text{BH}} \gtrsim 2$ , but near  $x_D$  the DF flattens, as required for the integrals in equation (4) to converge at high energies (Bahcall & Wolf 1977). Large slopes at intermediate energies are allowed by these equations, and arise when a population of massive objects with a low number density exists, as is the case in our model. At low energies the massive objects sink effectively to the center by dynamical friction. At high energies the massive objects dominate the dynamics, decouple from the lighter objects, and form an  $\alpha = 7/4$  “mini-cusp”. This process is reminiscent of the Spitzer instability in globular clusters, where SBHs decouple from the other stars (Spitzer & Hart 1971; Khalisi et al. 2006).

The probability for inspiral  $S_M(a)$  is shown in figure (2). Since the SBHs are more massive they lose energy to GWs at a higher rate than the other species and can spiral in from larger distances.

In figure (3) we show the cumulative rates of successful inspiral (Eq. 8) for all CRs as a function of distance from the MBH. We summarize some results in table (1), where we also give the enclosed number of stars  $N_M(<a)$  within  $a$ .

#### 4. SUMMARY AND DISCUSSION

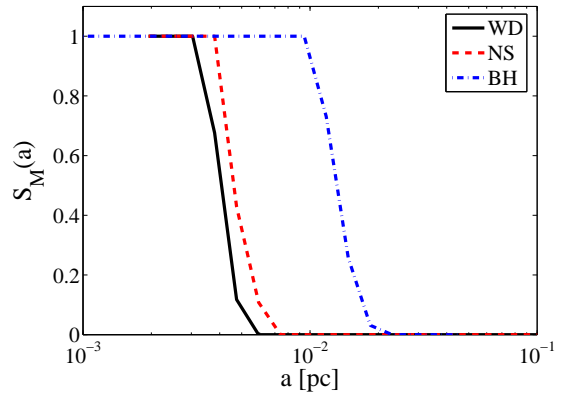


FIG. 2.— Probability of successful inspiral for a consumed star as a function of distance from the MBH for the CRs. BHs (dotted-dashed) can successfully spiral in from further distances than WDs (solid) and NSs (dashed) due to their higher masses.

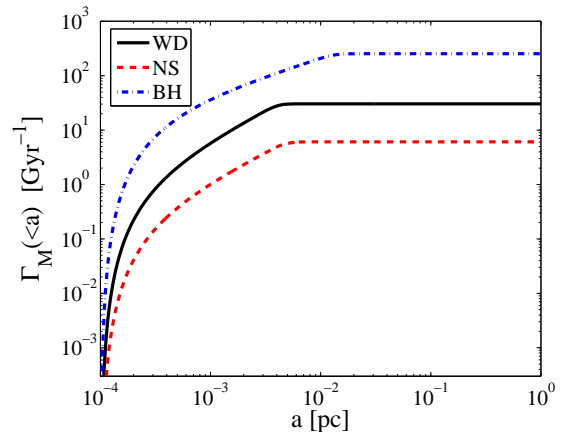


FIG. 3.— Cumulative rates as a function of  $a$  are dominated by BHs (dotted-dashed); WDs (solid) and NSs (dashed) contribute significantly less.

In our model, SBHs dominate the EMRI rate, in spite of their small number density at  $r_h$ . The combination of a very steep cusp ( $\alpha_{\text{BH}} \approx 2.0$ ) and a larger  $a_{\text{GW}}$  due to their larger mass leads to  $\Gamma_{\text{BH}} > (\Gamma_{\text{WD}}, \Gamma_{\text{NS}})$  per galaxy. We also note that the amplitude of the GWs is proportional to the stellar mass, so that the distance at which these objects can be observed is  $\sim 10$  times larger than that for WDs and NSs. Thus, SBHs will dominate the cosmic detection rate.

It is instructive to compare the EMRI rates we obtain here to those obtained by HA05, where mass-segregation was not explicitly included. For SBHs,  $\Gamma_{\text{BH}}$  is larger by a factor  $\sim 50$ . Part of the difference is that we assume here a larger total number of SBHs within the cusp (by a factor  $\sim 6$ ; we normalized the SBH number fraction at  $r_h$  to be  $C_{\text{BH}} = 10^{-3}$ , while HA05 assumed that the *enclosed* fraction of SBHs is  $10^{-3}$ ). More importantly, the steeper cusp leads to a higher capture rate (by a factor  $\sim 9$ , HA05, eq. [32]; HA05 assumed  $\alpha_{\text{BH}} = 1.75$ ). The BH cusp is much steeper than any of the cases studied by Bahcall & Wolf (1977), and in particular it is steeper than the cusp of a single mass population,  $\alpha = 7/4$  (Bahcall & Wolf 1976).

The rates  $\Gamma_{\text{WD}}$  and  $\Gamma_{\text{NS}}$  are also somewhat larger than those found by HA05. Here the difference originates mainly in the behavior of  $t_r$ : For WDs and NSs,  $t_r$  was assumed to be constant by HA05, as appropriate for a single mass popula-

tion with  $\alpha = 3/2$ . However, the interaction between SBHs and the other CRs leads to a decrease in  $t_r$  towards the MBH (Fig. 1). Using the analytical expressions by HA05, it can be shown that if  $n_M(r) \propto r^{-3/2}$ , and  $t_r \propto r^p$ , the successful inspiral rate is enhanced by  $(d_c/r_h)^{-3p/(3-2p)} \sim 10$  (for  $p = 0.5$ ) relative to the  $t_r = \text{const.}$  case, where  $d_c = [(85/3072)\sqrt{GM_\bullet}(M/M_\bullet)t_h]^{2/3}$ , see HA05 eq. (29).

The EMRI rates we found here are promising for the *LISA* detection rate (Barack & Cutler 2004b; Gair et al. 2004), in spite of the fact that more sources also imply a stronger background noise (Barack & Cutler 2004a).

We neglected here the effect of resonant relaxation (Rauch & Tremaine 1996; Rauch & Ingalls 1998), which can increase the EMRI rate by up to an order of magnitude (Hopman & Alexander 2006). A multi-mass analysis of RR has yet to be performed. In addition to *direct capture* of CRs, EMRI can occur following the formation of SBHs in accretion disks (Levin 2003), binary disruptions (Miller et al. 2005) and tidal capture followed by a super nova explosion of the captured star (Hopman & Portegies Zwart 2005). These other mechanisms lead to low eccentricity signals, whereas

direct capture leads to high eccentricities (HA05).

Our estimate of the number fraction of unbound SBHs is somewhat uncertain, in part because we neglected dynamical effects for unbound stars. We note that our estimate  $N_{\text{BH}}(< \text{pc}) \sim 1.6 \times 10^4$  is consistent with calculations by Miralda-Escudé & Gould (2000), who found  $N_{\text{BH}}(< \text{pc}) \sim 2.5 \times 10^4$ . Our Galactic Center contains a MBH of mass comparable to the MBH mass considered here (Ghez et al. 2005; Eisenhauer et al. 2005). Observational effects of a cluster of SBHs near the Galactic MBH include microlensing (Chanamé et al. 2001), X-ray emission (Pessah & Melia 2003), capture of massive stars by an exchange interaction (Alexander & Livio 2004) and deviations from Keplerian motion of luminous stars (Mouawad et al. 2005). Such effects could in principle be used to constrain the predicted densities.

TA is supported by ISF grant 295/02-1, Minerva grant 8563, and a New Faculty grant by Sir H. Djangoly, CBE, of London, UK.

#### APPENDIX

Because of the large range of energies, the natural way to integrate the Fokker-Planck equation is to divide the energy range into equal logarithmic intervals. For convenience we give here the equations in terms of the logarithmic distance variable  $z = \ln(1 + x/\lambda)$ . The Fokker-Planck equation without sink terms is then written as

$$\begin{aligned} \frac{\partial g_M(z, \tau)}{\partial \tau} = & -\frac{M}{M_\star} (e^z - 1)^{5/2} e^{-z} \times \\ & \sum_{M'} \frac{M'}{M_\star} \frac{\partial}{\partial z} \left[ (e^z - 1)^{-3/2} g_M(z) [g_{M'}(z) - g_{M'}(-\infty)] + g_M(z) \int_z^{z^D} dz' (e^{z'} - 1)^{-3/2} \frac{\partial g_{M'}(z')}{\partial z'} \right. \\ & \left. - \frac{M'}{M} (e^z - 1)^{-3/2} e^{-z} \frac{\partial g_M(z)}{\partial z} \int_{-\infty}^z dz' e^{z'} g_{M'}(z') - \frac{M'}{M} e^{-z} \frac{\partial g_M(z)}{\partial z} \int_z^{z^D} dz' e^{z'} (e^{z'} - 1)^{-3/2} g_{M'}(z') \right]. \quad (1) \end{aligned}$$

The logarithmic expressions for the sink term (eq. 6) can be included directly by replacing  $x \rightarrow \lambda(e^z - 1)$ .

#### REFERENCES

- Alexander, T. 2005, *Phys. Rep.*, 419, 65  
 Alexander, T. & Hopman, C. 2003, *ApJ*, 590, L29  
 Alexander, T. & Livio, M. 2004, *ApJ*, 606, L21  
 Alexander, T. & Morris, M. 2003, *ApJ*, 590, L25  
 Bahcall, J. N. & Wolf, R. A. 1976, *ApJ*, 209, 214  
 —. 1977, *ApJ*, 216, 883  
 Barack, L. & Cutler, C. 2004a, *Phys. Rev. D*, 70, 122002  
 —. 2004b, *Phys. Rev. D*, 69, 082005  
 Baumgardt, H., Hopman, C., Portegies Zwart, S., & Makino, J. 2005, *ArXiv Astrophysics e-prints*, astro-ph/0511752  
 Baumgardt, H., Makino, J., & Ebisuzaki, T. 2004, *ApJ*, 613, 1143  
 Chanamé, J., Gould, A., & Miralda-Escudé, J. 2001, *ApJ*, 563, 793  
 Cohn, H. & Kulsrud, R. M. 1978, *ApJ*, 226, 1087  
 Eisenhauer, F. et al. 2005, *ApJ*, 628, 246  
 Ferrarese, L. & Merritt, D. 2000, *ApJ*, 539, L9  
 Frank, J. & Rees, M. J. 1976, *MNRAS*, 176, 633  
 Freitag, M. 2001, *Classical and Quantum Gravity*, 18, 4033  
 —. 2003, *ApJ*, 583, L21  
 Freitag, M. & Benz, W. 2002, *A&A*, 394, 345  
 —. 2005, *MNRAS*, 245  
 Gair, J. R., Barack, L., Creighton, T., Cutler, C., Larson, S. L., Phinney, E. S., & Vallisneri, M. 2004, *Classical and Quantum Gravity*, 21, 1595  
 Gebhardt, K. et al. 2000, *ApJ*, 539, L13  
 Genzel, R. et al. 2003, *ApJ*, 594, 812  
 Ghez, A. M., Salim, S., Hornstein, S. D., Tanner, A., Lu, J. R., Morris, M., Becklin, E. E., & Duchêne, G. 2005, *ApJ*, 620, 744  
 Hils, D. & Bender, P. L. 1995, *ApJ*, 445, L7  
 Hopman, C. & Alexander, T. 2005, *ApJ*, 629, 362  
 —. 2006, *ArXiv Astrophysics e-prints*, astro-ph/0601161  
 Hopman, C. & Portegies Zwart, S. 2005, *MNRAS*, 363, L56  
 Hopman, C., Portegies Zwart, S. F., & Alexander, T. 2004, *ApJ*, 604, L101  
 Ivanov, P. B. 2002, *MNRAS*, 336, 373  
 Khalisi, E., Amaro-Seoane, P., & Spurzem, R. 2006, *ArXiv Astrophysics e-prints*, astro-ph/0602570  
 Levin, Y. 2003, *arXiv*, available at <http://xxx.lanl.gov/abs/astro-ph/0307084>  
 Lightman, A. P. & Shapiro, S. L. 1977, *ApJ*, 211, 244  
 Magorrian, J. & Tremaine, S. 1999, *MNRAS*, 309, 447  
 Miller, M. C., Freitag, M., Hamilton, D. P., & Lauburg, V. M. 2005, *ApJ*, 631, L117  
 Miralda-Escudé, J. & Gould, A. 2000, *ApJ*, 545, 847  
 Mouawad, N., Eckart, A., Pfalzner, S., Schödel, R., Moulta, J., & Spurzem, R. 2005, *Astronomische Nachrichten*, 326, 83  
 Pessah, M. & Melia, F. 2003, *ApJ*, 585, L29  
 Peters, P. C. 1964, *Physical Review*, 136, 1224  
 Rauch, K. P. & Ingalls, B. 1998, *MNRAS*, 299, 1231  
 Rauch, K. P. & Tremaine, S. 1996, *New Astronomy*, 1, 149  
 Rubbo, L. J., Holley-Bockelmann, K., & Finn, L. S. 2006, *ArXiv Astrophysics e-prints*, astro-ph/0602445  
 Sigurdsson, S. & Rees, M. J. 1997, *MNRAS*, 284, 318  
 Spitzer, L. J. & Hart, M. H. 1971, *ApJ*, 164, 399  
 Syer, D. & Ulmer, A. 1999, *MNRAS*, 306, 35  
 Tremaine, S. et al. 2002, *ApJ*, 574, 740